ALZHEIMER'S DISEASE

APOE4 disrupts intracellular lipid homeostasis in human iPSC-derived glia

Grzegorz Sienski[1]*†, Priyanka Narayan[1,2,3]*, Julia Maeve Bonner[1,2]*, Nora Kory[1], Sebastian Boland[4], Aleksandra A. Arczewska[5†], William T. Ralvenius[2], Leyla Akay[2], Elana Lockshin[2], Liang He[6], Blerta Milo[2], Agnese Graziosi[2], Valeriya Baru[1‡], Caroline A. Lewis[1], Manolis Kellis[7,8], David M. Sabatini[1,7,9,10,11], Li-Huei Tsai[2,7§], Susan Lindquist[1,9,10‖]

The *E4* allele of the apolipoprotein E gene (*APOE*) has been established as a genetic risk factor for many diseases including cardiovascular diseases and Alzheimer's disease (AD), yet its mechanism of action remains poorly understood. APOE is a lipid transport protein, and the dysregulation of lipids has recently emerged as a key feature of several neurodegenerative diseases including AD. However, it is unclear how APOE4 perturbs the intracellular lipid state. Here, we report that *APOE4*, but not *APOE3*, disrupted the cellular lipidomes of human induced pluripotent stem cell (iPSC)–derived astrocytes generated from fibroblasts of *APOE4* or *APOE3* carriers, and of yeast expressing human *APOE* isoforms. We combined lipidomics and unbiased genome-wide screens in yeast with functional and genetic characterization to demonstrate that human APOE4 induced altered lipid homeostasis. These changes resulted in increased unsaturation of fatty acids and accumulation of intracellular lipid droplets both in yeast and in *APOE4*-expressing human iPSC-derived astrocytes. We then identified genetic and chemical modulators of this lipid disruption. We showed that supplementation of the culture medium with choline (a soluble phospholipid precursor) restored the cellular lipidome to its basal state in *APOE4*-expressing human iPSC-derived astrocytes and in yeast expressing human *APOE4*. Our study illuminates key molecular disruptions in lipid metabolism that may contribute to the disease risk linked to the *APOE4* genotype. Our study suggests that manipulating lipid metabolism could be a therapeutic approach to help alleviate the consequences of carrying the *APOE4* allele.

INTRODUCTION

Genome-wide association studies implicate lipid metabolism in a number of late-onset neurodegenerative diseases, including Alzheimer's disease (AD) (*1*–*5*). The accumulation of lipid (adipose saccules) in glia is a pathologically defining feature of AD (*6*). The most highly validated genetic risk factor for late-onset AD is the ε4 allele of the *APOE* gene (*APOE4*). *APOE* encodes a lipid-carrier protein that is a key component of many lipoprotein particles (*7*–*9*).

The human gene encoding *APOE* is polymorphic with three common coding variants (isoforms) differing from one another by two amino acids: ε3 (*APOE3*), ε4 (*APOE4*), and ε2 (*APOE2*) (*10*). The *APOE4* genotype is the primary genetic risk factor for late-onset AD (*11*–*13*), is associated with cardiovascular diseases (*14*, *15*), increases risk for metabolic syndrome (*16*), and is linked with decreased life span (*17*). The presence of *APOE4* lowers the age of AD onset and increases the lifetime risk for developing the disease in a gene dose-dependent manner (*18*).

Apolipoprotein E (APOE) is a component of many lipoprotein particles and serves as a ligand for membrane receptors that mediate lipoprotein uptake (*7*–*9*). APOE4 has been suggested to contribute to AD pathogenesis by modulating multiple pathways including lipid transport and metabolism (*19*); however, the ways in which APOE4 alters the lipidome of cells remain unknown. In this study, we characterized the lipidome of *APOE4*-expressing human astrocytes differentiated from induced pluripotent stem cells (iPSCs) generated from fibroblasts from both *APOE4* and *APOE3* carriers (*20*). We found that human iPSC-derived *APOE4* astrocytes accumulated unsaturated triacylglycerides stored in lipid droplets to a greater extent than did their isogenic *APOE3* counterparts. Using the conservation of lipid metabolism pathways between yeast and human cells (*21*–*24*) we established a yeast model where the expression of human *APOE4*, but not human *APOE3*, by yeast induced the accumulation of lipid droplets and increased unsaturation of triacylglycerides in a similar manner to human iPSC-derived *APOE4* astrocytes. Lipid droplet accumulation was accompanied by a specific growth defect in *APOE4*-expressing yeast. Loss-of-function genetic screens revealed that perturbations in a lipogenic transcriptional program uncoupled *APOE4* from its cytotoxic effects. Promoting synthesis of the membrane lipid phosphatidylcholine by supplementing cell cultures with choline reversed the abnormal lipid unsaturation and lipid droplet accumulation in both *APOE4*-expressing yeast and human iPSC-derived astrocytes.

[1]Whitehead Institute for Biomedical Research, Cambridge, MA 02142, USA. [2]Picower Institute for Learning and Memory, Department of Brain and Cognitive Sciences, MIT, Cambridge, MA 02139, USA. [3]Genetics and Biochemistry Branch, NIDDK, National Institutes of Health, Bethesda, MD 20814, USA. [4]Department of Molecular Metabolism, Harvard T.H. Chan School of Public Health, Boston, MA 02115, USA. [5]Department of Stem Cell and Regenerative Biology, Harvard University, Cambridge, MA 02138, USA. [6]Duke University, Durham, NC 27708, USA. [7]Broad Institute of Harvard and Massachusetts Institute of Technology, Cambridge, MA 02142, USA. [8]Computer Science and Artificial Intelligence Laboratory, Massachusetts Institute of Technology, Cambridge, MA 02139, USA. [9]Massachusetts Institute of Technology, Cambridge, MA 02142, USA. [10]Howard Hughes Medical Institute, Cambridge, MA 02139, USA. [11]Koch Institute for Integrative Cancer Research and Massachusetts Institute of Technology, Department of Biology, Cambridge, MA 02139, USA.
*These authors contributed equally to this work.
†Present address: Discovery Biology, Discovery Sciences, BioPharmaceuticals R&D, AstraZeneca, Gothenburg, Sweden.
‡Present address: Q-State Biosciences, Cambridge, MA 02139, USA.
§Corresponding author. Email: lhtsai@mit.edu
‖Deceased.

RESULTS

Human iPSC-derived APOE4-expressing astrocytes display intracellular lipid dysregulation

We first characterized the impact of the *APOE4* allele on the lipidome of human iPSC-derived astrocytes. In the brain, astrocytes are the major source of APOE (*25*) and have previously been reported to show *APOE4*-specific defects (*26*, *27*). We used two independent pairs of previously published isogenic iPSC lines, derived from either a parental *APOE3* or *APOE4* homozygote, that had been edited with CRISPR-Cas9 to make the corresponding *APOE3* or *APOE4* isogenic line. These lines were differentiated into astrocytes that expressed the astrocyte proteins GFAP (glial fibrillary acidic protein) and S100β (Fig. 1, A and B) (*27*).

We compared the lipid composition of the *APOE3*- and *APOE4*-expressing human iPSC-derived astrocytes by performing whole-cell lipidomic analysis using liquid chromatography–mass spectrometry (LC-MS) (*28*, *29*). We observed a minor change in phospholipid content and a much larger increase in triacylglycerides in *APOE4*-expressing human iPSC-derived astrocytes compared with *APOE3*-expressing human iPSC-derived astrocytes (Fig. 1C). We also observed that the degree of unsaturation of the fatty acids attached to triacylglycerides in *APOE4*-expressing astrocytes was higher than that in *APOE3*-expressing astrocytes (Fig. 1D). Triacylglycerides, along with other neutral lipids such as cholesterol esters, are stored in cytoplasmic organelles called lipid droplets (*30*). We therefore stained our isogenic astrocytes using a lipophilic dye, LipidTox, that labels neutral lipids (*31*). After 2 weeks in culture, we observed that *APOE4* astrocytes accumulated a greater number of lipid droplets than did their *APOE3* counterparts (Fig. 1E), which was accompanied by accumulation of a lipid droplet–resident protein, Perilipin-2 (Fig. 1F) (*32*). We validated these findings in an additional pair of isogenic iPSC lines (fig. S1A), again observing increased accumulation of lipid droplets in *APOE4* astrocytes as compared with *APOE3* astrocytes (fig. S1B).

APOE4 alters the lipid burden in microglia

To address whether the *APOE4*-associated intracellular lipid accumulation was present in other cell types, we examined microglia, which play a key role in AD (*33*) and were recently described to accumulate lipids in aged mice (*4*). We derived *APOE3* and *APOE4* microglia from our isogenic iPSC lines (fig. S1C) and measured their lipid droplet content. We observed fewer lipid droplet–bearing microglia in culture than we observed for astrocytes under similar culture conditions. Even so, *APOE4* microglia showed more lipid droplet–positive cells per well (fig. S1E, left) than did *APOE3* microglia. After 2 weeks of culture in minimal medium, *APOE4* microglia displayed a trend toward increased lipid droplet numbers per cell when compared with *APOE3* microglia (fig. S1D). Stimulation of the cultures by interferon-γ resulted in increased numbers of lipid droplet–bearing cells for both *APOE3* and *APOE4* cells (fig. S1E, right). These findings suggested that *APOE4*-associated lipid dysregulation occurred in multiple glial cell types.

Gene expression in brain tissue from individuals with the *APOE4* allele suggests dysregulated lipid metabolism

To determine whether our iPSC-derived human astrocyte cultures reflected *APOE4*-related dysfunction present in human brains, we examined transcriptomic data from postmortem human brain samples

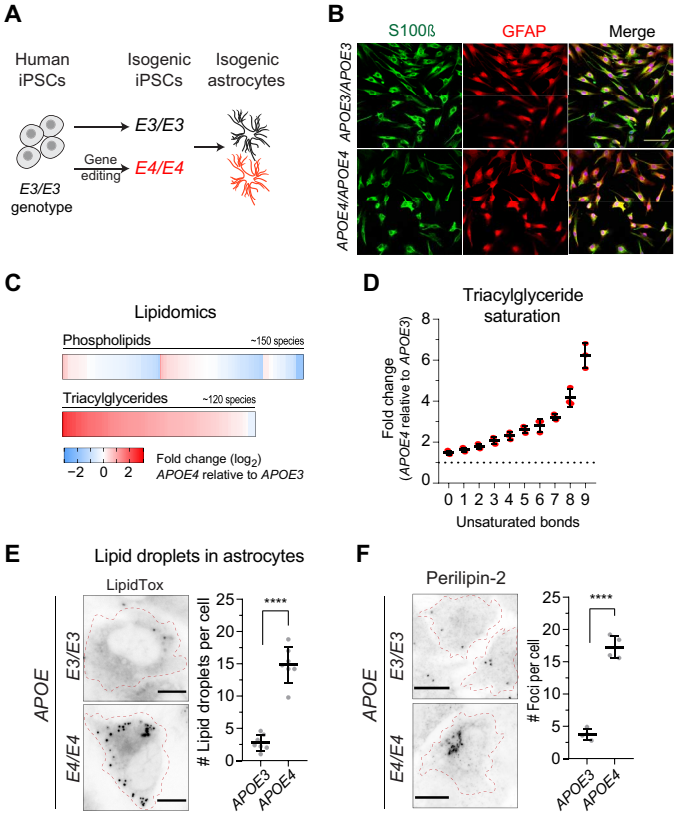

Fig. 1. An increase in lipid droplets in *APOE4*-expressing human iPSC-derived astrocytes. (**A**) The schematic shows the differentiation of isogenic astrocytes of the *APOE3/APOE3* and *APOE4/APOE4* genotypes from human iPSCs. (**B**) Representative fluorescence microscopy images ($N = 3$ replicates) of *APOE3/APOE3* and *APOE4/APOE4* isogenic astrocytes stained with antibodies against S100β and GFAP (scale bar, 100 μm). (**C**) Heatmap showing the fold change ($\log_2$) in abundance of phospholipids (~150 lipid species) and triacylglycerides (~120 species) between isogenic *APOE4/APOE4* and *APOE3/APOE3* human iPSC-derived astrocytes. (**D**) Graph shows fold change difference in the number of unsaturated bonds in fatty acids attached to triacylglycerides between isogenic *APOE4/APOE4* and *APOE3/APOE3* human iPSC-derived astrocytes. For this analysis, we summed the number of unsaturated carbon bonds per triacylglyceride molecule. (**E**) Representative microscopy images of isogenic *APOE4/APOE4* and *APOE3/APOE3* human iPSC-derived astrocytes in culture stained with LipidTox. Quantification of the lipid droplet number per cell is shown in the right panel, with each dot representing an average of at least 20 cells in four wells analyzed ($N = 7$ independent replicates). Data are represented as means ± SD; $^{****}P \leq 0.0001$ by Student's *t* test. The dashed line denotes the boundaries of the cell (scale bars, 20 μm). (**F**) Representative microscopy images of isogenic *APOE4/APOE4* and *APOE3/APOE3* human iPSC-derived astrocytes in culture stained with an anti–Perilipin-2 antibody. Magnification is the same as in (E). Quantification of the Perilipin-2 foci per cell is shown in the right panel, with each dot representing an average of four wells with at least 20 cells analyzed ($N = 4$ independent replicates). Data are represented as means ± SD; $^{****}P \leq 0.0001$ by Student's *t* test.

characterized in the Genotype-Tissue Expression (GTEx) project, containing tissue-specific gene expression data for individuals of varying genotype, age, and cause of death. We explored the influence of the *APOE4* allele on lipid metabolic pathways, independent of disease state, by comparing the transcriptomic profiles of *APOE4* carriers with noncarriers across a Kyoto Encyclopedia of Genes and Genomes (KEGG)–based curated set of 609 lipid metabolism genes (fig. S1F and table S1); 529 genes were detected within the GTEx cortex dataset. Of the genes that were significantly differentially expressed

[false discovery rate (FDR) corrected $P < 0.05$] in *APOE4* carriers when compared with noncarriers, we identified up-regulated genes involved in the metabolism of neutral lipids and cholesterol (*FA2H*, *ACSL1*, *SQLE*, *HMGCR*, and *MVK*), as well as down-regulated genes involved in the metabolism of fatty acids and neutral lipids (*OLAH*, *CNEP1R1*, and *GPAM*) (fig. S1F). This analysis suggested that in the human cortex, *APOE4*-mediated perturbation of lipid metabolism could be detected in the transcriptome of *APOE4* carriers.

Expression of APOE4 in yeast recapitulates lipid defects identified in human astrocytes

To explore *APOE4*-associated lipid defects in an unbiased and genetically tractable manner, we used the remarkable conservation of lipid metabolism pathways across eukaryotes including baker's yeast, *Saccharomyces cerevisiae* (*21*, *23*, *24*, *34*).

We first established an *APOE* model in yeast that captured the lipid dysfunction that we observed in human cells. Our model used the human complementary DNA (cDNA) of *APOE3* and *APOE4*, directed to the secretory pathway using the signal sequence from *S. cerevisiae* Kar2p (fig. S2A), to mirror the localization of APOE in human cells (*35*, *36*). The constructs were driven by tunable transcriptional activation mediated by β-estradiol (*37*). We found that expression of human *APOE4*, but not human *APOE3*, induced the accumulation of lipid droplets in yeast grown in minimal culture medium (Fig. 2A), just as we had observed for *APOE4*-expressing human iPSC-derived astrocytes. The *APOE4* yeast strain also accumulated the lipid droplet–resident proteins, Erg6p and Faa4p (fig. S2B) (*38*). Yeast cells expressing other neurodegenerative disease–related proteins, Aβ1-42 and TDP-43, showed only a minor increase in accumulation of the neutral lipid dye, BODIPY 493/503, compared with *APOE4*-expressing yeast (fig. S2C). The extent of lipid accumulation and dysregulation therefore was a unique feature of *APOE4*-expressing cells.

We performed lipid extraction and lipidomic analyses of *APOE3*- and *APOE4*-expressing yeast, observing an increase in the amount of triacylglycerides (Fig. 2B) and the unsaturated fatty acids attached to them (fig. S2D), similar to what we observed in *APOE4*-expressing human iPSC-derived astrocytes. Thus, expression of *APOE4* in our yeast model induced similar lipid defects to those observed in human iPSC-derived astrocytes and therefore could be used to probe the genetics underlying this effect.

Loss-of-function yeast genetic screens reveal suppressors of APOE4-mediated lipid defects

The disruption in lipid homeostasis in *APOE4*-expressing yeast was accompanied by an isoform-specific growth defect when the yeast were grown on either solid medium (Fig. 2C) or in liquid synthetic complete supplement mixture medium (Fig. 2D and fig. S3A). This growth defect scaled with expression of *APOE4*, where increasing amounts of APOE4 protein correlated with a reduction in the growth rate (fig. S3B). This effect was not observed for *APOE3*-expressing yeast (fig. S3C).

Given that *APOE4*-expressing yeast exhibited the lipid homeostasis defects observed in *APOE4*-expressing human iPSC-derived astrocytes, we performed loss-of-function genetic screens among the nonessential genes in the yeast genome to identify genetic suppressors of the *APOE4*-induced growth phenotype (*39*, *40*). We performed two independent screens with the *APOE4* gene expressed either from a cassette integrated into the yeast genome or from a centromeric plasmid (fig. S3D). The gene deletion strains that exhibited unperturbed growth despite the expression of *APOE4* (Fig. 2E and fig. S3E) were enriched for genes whose protein products are associated with the endoplasmic reticulum (fig. S3F), with many genes reported to genetically interact with each other (*41*). Our top hits were *OPI1*, *MGA2*, and *UBX2*, which all encode proteins that regulate lipid metabolism (Fig. 2, E and F) (*42*, *43*). Mga2p and Ubx2p act as sensors for fatty acid saturation (*42*, *44*–*46*), and Opi1p works as a sensor of phospholipid composition (*47*–*49*). We focused on *MGA2* and *OPI1* and found that deletion of neither *MGA2* nor *OPI1* altered the amounts of APOE4 protein (Fig. 2G). Given the established role of Mga2p and Opi1p in yeast lipid metabolism (*42*, *47*, *48*, *50*), our results reaffirmed that the *APOE4*-associated growth impediment in yeast stemmed from abnormal lipid metabolism.

An imbalance in lipid saturation is the primary contributor to APOE4-associated lipid defects in yeast

Both Ubx2p and Mga2p control the stability and expression of the only fatty acyl-CoA (coenzyme A) desaturase in yeast, *OLE1* (*42*, *51*, *52*). Because the gene encoding the Ole1p desaturase is an essential gene in yeast, it was not present in the library we used for our loss-of-function genetic screens. We engineered an *mga2*Δ yeast strain in which *APOE4* expression was no longer associated with a growth defect. We observed that complementation of the *mga2*Δ strains with either *MGA2* or *OLE1* under control of a constitutively active promoter rendered yeast cells sensitive again to *APOE4* expression (fig. S3G). Chemical inhibition of Ole1p with a small molecule (ECC145) (*53*) restored the growth of *APOE4*-expressing yeast cells in a dose-dependent manner without affecting the growth of *GFP*- or *APOE3*-expressing cells (Fig. 2H). Last, we asked whether *MGA2* was involved in the *APOE4*-mediated accumulation of lipid droplets. We measured the BODIPY 493/503 signal in the *mga2*Δ strain and found that the signal did not accumulate (Fig. 2I).

Lipid droplets act to buffer against lipotoxicity by sequestering free fatty acids (FFAs) as triacylglycerides (*54*). To test whether a high burden of triacylglycerides altered the lipid buffering capacity of *APOE4*-expressing yeast cells, we treated this strain with oleic acid (C18:1), an unsaturated FFA. We found that whereas the growth of both wild-type and *APOE3*-expressing yeast was not affected by the addition of this FFA, the growth defect in the *APOE4*-expressing yeast was exacerbated by addition of oleic acid (fig. S3H).

Choline supplementation is sufficient to rescue APOE4-induced lipid defects in yeast

Cellular lipid metabolism is shaped by both genes and environment (*55*). We asked whether yeast medium differing in nutrient content could modify the growth of *APOE4*-expressing or *APOE3*-expressing yeast. Whereas yeast grown in synthetic medium displayed a growth difference between *APOE3*-expressing and *APOE4*-expressing cells, yeast grown in a rich medium (yeast extract–peptone) did not (fig. S4, A and B). This observation suggested that the *APOE4* slow-growth phenotype depended on nutrient availability. This effect was specific to *APOE4*-expressing yeast, as yeast expressing other proteins (Aβ1-42 and TDP43) displayed a clear growth disadvantage in both synthetic medium and yeast extract–peptone medium (fig. S4A). This finding suggested that environmental factors could modify *APOE4* phenotypes in yeast.

Given that one of our top genetic screen hits, *OPI1*, is a negative regulator of phospholipid synthesis (*48*, *49*, *56*), we asked whether

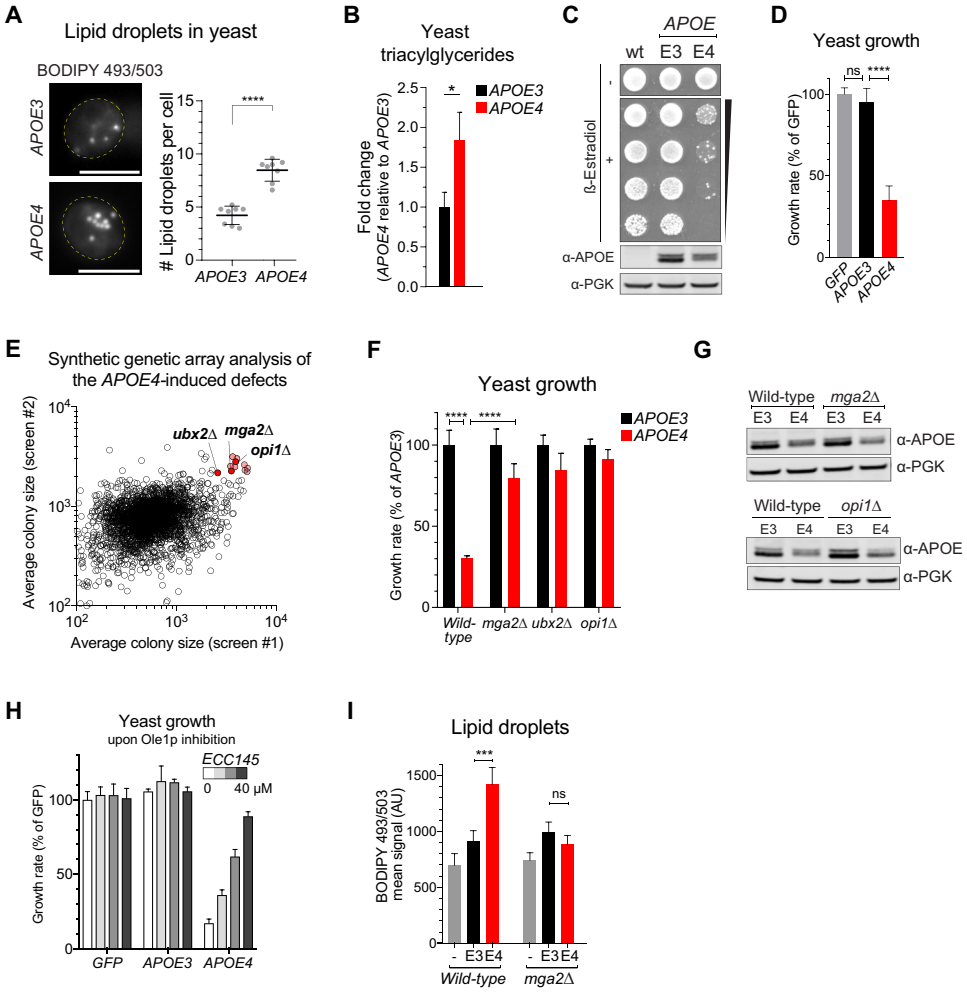

Fig. 2. Lipid homeostasis is perturbed in yeast expressing human *APOE4*. (**A**) Representative fluorescence microscopy images of yeast expressing human *APOE3* or *APOE4* stained with BODIPY 493/503 stain for lipid droplets after growth in synthetic medium (scale bars, 5 μm). Quantification of the number of lipid droplets in yeast is shown in the right panel ($N = 8$ experiments, each with at least 30 yeast cells analyzed). Data are represented as means ± SD; $^{****}P \leq 0.0001$ by Student's *t* test. The dashed line denotes the boundaries of the yeast cell. (**B**) Bar graph shows fold change difference in intracellular triacylglycerides between *APOE3*-expressing and *APOE4*-expressing yeast cells. Data represent means ± SD; $n = 2$ independently grown colonies; $^{*}P \leq 0.05$ by Student's *t* test. (**C**) Yeast growth assay on agar plates containing synthetic complete medium with (+) or without (–) β-estradiol to induce the expression of human *APOE3* or *APOE4*. Representative agar plate shows fivefold dilutions of yeast cultures. Western blot shows yeast samples collected from the agar plate after 8 hours of β-estradiol induction of *APOE3* or *APOE4* expression. APOE3 and APOE4 were probed with anti-APOE antibody; anti-PGK1 antibody was used as a loading control. (**D**) Bar graph shows growth of wild-type yeast expressing *GFP* or yeast expressing human *APOE3* or *APOE4* cultured in synthetic complete medium for 24 hours. Data are normalized to the growth rate of the green fluorescent protein (GFP)–expressing strain (control) and represented as means ± SD; $n = 3$ independent yeast colonies with at least two technical replicates. ns, nonsignificant; $P > 0.05$ and $^{****}P \leq 0.0001$ by Student's *t* test. (**E**) A scatter plot from two independent loss-of-function genetic screens showing the average colony size of yeast deletion strains with loss of individual nonessential genes and expressing human *APOE4*. Each circle represents data averaged from four technical replicates. Yeast strains with variability higher than SD > 25% between technical replicates were removed, resulting in ~2800 genes assayed. (**F**) Bar graph shows the growth of yeast expressing *APOE4* compared with those expressing *APOE3* for a wild-type strain and for *mga2*Δ, *ubx2*Δ, and *opi1*Δ strains. Data are represented as means ± SD; $n = 3$ independent yeast colonies with at least two technical replicates each. $P > 0.05$ and $^{****}P \leq 0.0001$ by Student's *t* test. (**G**) Western blot of whole-cell extracts of wild-type and *MGA2*-null yeast (top) and wild-type and *OPI1*-null yeast (bottom) showing expression of human APOE3 and APOE4, with PGK1 as the loading control. (**H**) Bar graph shows the growth rate of *APOE3*- and *APOE4*-expressing yeast treated with 10, 20, or 40 μM ECC145 (an Ole1p inhibitor) or vehicle [dimethyl sulfoxide (DMSO)]. The data are normalized to the growth of a control untreated yeast strain expressing GFP. Data are represented as means ± SD; $n = 3$ independent yeast colonies with at least two technical replicates each. (**I**) Bar graph shows the mean signal of BODIPY 498/503 stain measured by fluorescence-based cell cytometry in yeast expressing human *APOE3* or *APOE4* for a wild-type strain or a *MGA2*-null strain. Data represent means ± SD; $n = 3$ independent yeast colonies with at least two technical replicates each. $^{***}P \leq 0.001$ by Student's *t* test. AU, arbitrary units.

the soluble precursors of phospholipid synthesis, ethanolamine and choline (*57*), could modulate the *APOE4*-related growth defect (*58*). While ethanolamine did not influence growth of yeast expressing *APOE4*, addition of choline salts (choline chloride or choline bitartrate) to synthetic yeast medium was sufficient to suppress the *APOE4*-associated growth defect (Fig. 3A) in a dose-dependent manner (Fig. 3B). Similar to the genetic rescue observed upon deletion of *MGA2*, choline supplementation did not simply decrease APOE4 protein (Fig. 3C) but rather uncoupled the presence of APOE4 from its growth-perturbing effects. Furthermore, the observed rescue was specific to *APOE4*, as synthetic medium supplemented with choline did not rescue the growth defect in yeast expressing Aβ1-42 (fig. S4C). Given that choline is a growth-limiting factor in *APOE4*-expressing yeast cultured in synthetic medium, we measured intracellular amounts of choline and the choline derivatives, phosphocholine and glycerophosphocholine. We found that, compared with *APOE3*-expressing yeast, *APOE4*-expressing yeast grown in synthetic medium contained elevated concentrations of these molecules (fig. S4D).

Choline (trimethylamine) serves as the head group for phosphatidylcholines and sphingomyelins and functions as a signaling molecule and methyl donor (*59*). Both yeast and human cells can generate phosphatidylcholine by the choline-dependent Kennedy pathway or the choline-independent phosphatidylethanolamine methylation pathway (fig. S4E) (*57*, *60*). To understand which of these biosynthesis pathways was relevant to choline-dependent rescue of the

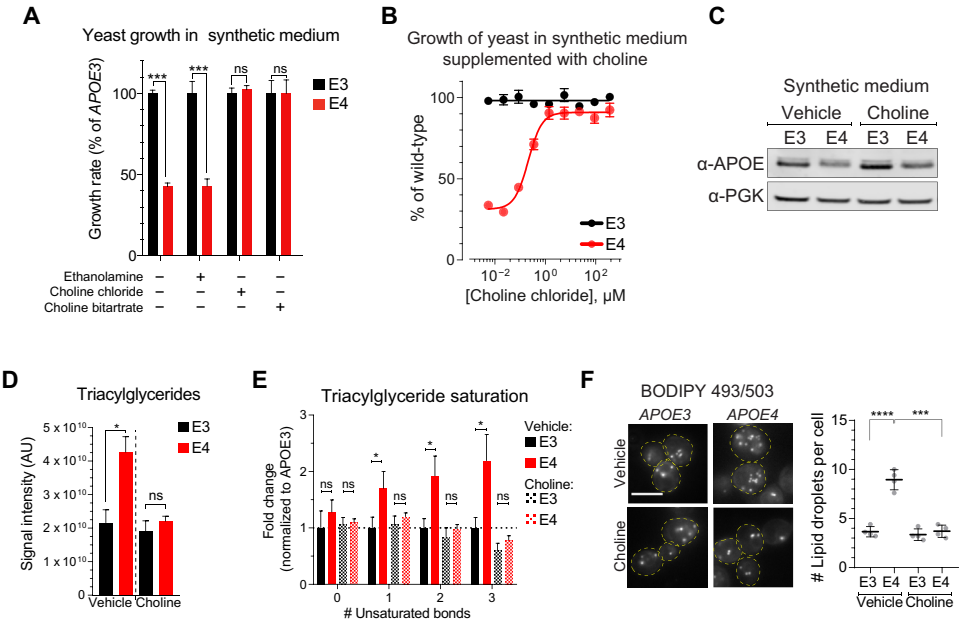

Fig. 3. Choline supplementation rescues *APOE4*-mediated lipid defects in yeast. (**A**) Relative growth of *APOE4*-expressing yeast in synthetic medium supplemented with ethanolamine (1 mM), choline chloride (1 mM), or choline bitartrate (100 μg/ml). Data are shown relative to the growth of the *APOE3*-expressing strain. Data are represented as means ± SD; $n = 3$ independent yeast colonies with at least two technical replicates each. $P > 0.05$ and $^{***}P \leq 0.001$ by Student's *t* test. (**B**) Graph shows growth of *APOE4*- and *APOE3*-expressing yeast strains normalized to a wild-type strain after culture in synthetic medium supplemented with choline chloride. Data represent measurements of three independent yeast colonies with at least two technical replicates each. (**C**) Western blot of whole-cell extracts of yeast expressing *APOE3* or *APOE4* cultured in synthetic medium with or without choline supplementation (1 mM), with PGK1 serving as loading control. (**D**) Bar graph shows intracellular triacylglycerides in *APOE3*- and *APOE4*-expressing yeast cells grown in synthetic medium with choline (1 mM) supplementation or vehicle as control. Data represent means ± SD; $n = 3$ independent yeast colonies. $P > 0.05$ and $^{*}P \leq 0.05$ by Student's *t* test. (**E**) Bar graph shows the fold change difference in intracellular triacylglycerides in *APOE3*- and *APOE4*-expressing yeast cells grown in synthetic medium supplemented with choline (1 mM) or vehicle as control. Triacylglycerides were stratified by the total number of unsaturated bonds present in the attached fatty acids. Data represent means ± SD; $n = 3$ independent yeast colonies measured. $P > 0.05$ and $^{*}P \leq 0.05$ by Student's *t* test. (**F**) Representative fluorescence microscopy images of *APOE3*- and *APOE4*-expressing yeast stained with BODIPY 493/503 stain for lipid droplets after growth in synthetic medium supplemented with choline (1 mM) or vehicle as control. Scale bar, 5 μm. Yellow dashed lines demarcate individual yeast cells. Quantification of the number of lipid droplets is shown in the right panel ($N = 4$ experiments, each with at least 30 yeast cells analyzed). Data are represented as means ± SD. $^{***}P \leq 0.001$ and $^{****}P \leq 0.0001$ by analysis of variance (ANOVA).

APOE4 phenotypes, we deleted every enzyme in the phosphatidylcholine synthesis or phosphatidylethanolamine synthesis pathways (*57*). As expected, the genetic ablation of the phosphatidylethanolamine synthesis pathway did not affect the growth of *APOE3*- or *APOE4*-expressing strains cultured in nutrient-rich yeast extract–peptone medium (fig. S4F). In contrast, the deletion of every enzyme acting in the phosphatidylcholine synthesis pathway rendered *APOE4*-expressing strains slow-growing, despite being grown in the nutrient-rich yeast extract–peptone medium (fig. S4F). We also observed differential growth between *APOE3*-expressing and *APOE4*-expressing strains upon deletion of *HNM1*, a transporter that carries choline and ethanolamine into yeast cells (*61*). We therefore concluded that without *HNM1*, *CKI1*, *PCT1*, and *CPT1*, yeast cells could not process the excess choline delivered by the yeast extract–peptone medium to support the growth of *APOE4*-expressing yeast. Thus, the Kennedy pathway was necessary to sustain the growth of *APOE4*-expressing yeast.

APOE4-expressing yeast cells show elevated levels of phosphatidylcholine

To characterize the broader impact of choline supplementation on cellular lipid composition, we used LC-MS–based lipidomics to analyze lipids from *APOE3*- and *APOE4*-expressing yeast grown in either synthetic medium alone or synthetic medium supplemented with choline. Along with the previously observed increases in triacylglycerides and unsaturated fatty acids upon *APOE4* expression (Fig. 2B and fig. S2D), *APOE4*-expressing yeast cells also displayed elevated total phosphatidylcholine when cultured in minimal synthetic medium (fig. S4G). These data suggested that *APOE4*-expressing yeast cells may have engaged the phosphatidylcholine synthesis pathway to provide an alternate sink for unsaturated fatty acids that would otherwise have accumulated in triglycerides and lipid droplets. Choline supplementation decreased both intracellular triacylglycerides (Fig. 3D) and the quantities of unsaturated fatty acids attached to triacylglycerides in *APOE4*-expressing yeast to levels found in *APOE3*-expressing cells (Fig. 3E). In line with this result, choline supplementation also prevented lipid droplet accumulation in *APOE4*-expressing yeast (Fig. 3F).

Targeting of lipid desaturation and triacylglyceride synthesis modifies APOE4-mediated lipid accumulation in human iPSC-derived astrocytes

We then investigated whether our findings in yeast could be reproduced in human iPSC-derived astrocytes. Examining previously published transcriptomes of human iPSC-derived astrocytes (*27*), we noted that *APOE4*-expressing human iPSC-derived astrocytes showed a decrease in transcripts of fatty acid desaturases including *SCD* and *FADS2* (fig. S5A), suggesting that, as in yeast, fatty acid saturation enzymes could be mediating *APOE4*-associated lipid defects. We chemically interrogated this pathway by treating *APOE4*-expressing human iPSC-derived astrocytes in culture with a small-molecule inhibitor of SCD1 (A939572) (*62*), the human homolog of yeast Ole1p. Inhibition of SCD1 resulted in a reduced number of lipid droplets (Fig. 4A) analogous to our finding in *APOE4*-expressing yeast (Fig. 2I).

Triacylglyceride and phosphatidylcholine synthesis pathways share a common substrate, diacylglycerol (fig. S5B). We hypothesized that chemically impairing the synthesis of triacylglycerides so that diacylglycerol served as a substrate only for the synthesis of phospholipids would ameliorate the lipid droplet burden in *APOE4*-expressing human iPSC-derived astrocytes. We treated *APOE4*-expressing human

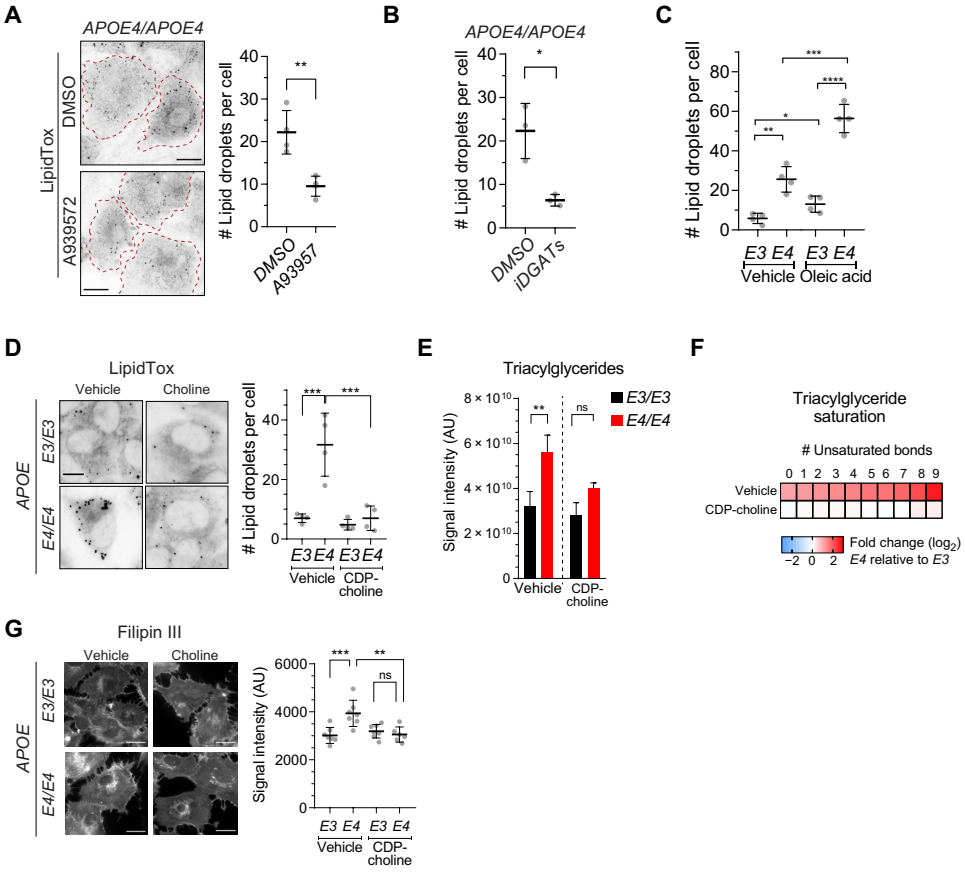

Fig. 4. Modification of APOE4-induced lipid droplet accumulation in human iPSC-derived astrocytes. (**A**) Representative microscopy images of *APOE4/APOE4* human iPSC-derived astrocytes treated with A939572 (an inhibitor of stearoyl-CoA desaturase-1, 100 nM) or DMSO vehicle control, stained with LipidTox. Quantification of the lipid droplet number per cell is shown in the right panel. Each dot is an average of four wells, with at least 20 cells measured ($N = 4$ independent replicates). Data are represented as means ± SD; $^{**}P \leq 0.01$ by Student's *t* test. Scale bar, 25 μm. The red dashed lines denote the boundaries of the cells. (**B**) Quantification of the lipid droplet number per cell in *APOE4/APOE4* human iPSC-derived astrocytes treated with a combination of small-molecule inhibitors of diacylglycerol *O*-acyltransferase 1 and 2 (iDGATs; 1 μM) or DMSO as vehicle control. Each dot is an average of ~50 cells analyzed. Data represent means ± SD. $^{*}P \leq 0.05$ by Student's *t* test. (**C**) Quantification of the number of lipid droplets in *APOE4- or APOE3*-expressing human iPSC-derived astrocytes treated with oleic acid (20 μM) or vehicle control ($N = 4$ experiments; each experiment imaged at least 20 cells). Data represent means ± SD. $^{*}P \leq 0.05$, $^{**}P \leq 0.01$, $^{***}P \leq 0.001$ by ANOVA with multiple comparisons. (**D**) Representative microscopy images of *APOE4- or APOE3*-expressing human iPSC-derived astrocytes stained with LipidTox after culture in medium supplemented with CDP-choline (100 μM) or vehicle as control. Quantification of the lipid droplet number per cell is shown in the right panel ($N = 4$ experiments, with at least 20 cells measured per experiment). Data represent means ± SD. $^{***}P \leq 0.001$ by ANOVA. (**E**) Bar graph shows intracellular triacylglycerides extracted from *APOE3*- or *APOE4*-expressing human iPSC-derived astrocytes grown in astrocyte culture medium supplemented with CDP-choline (100 μM) or vehicle as control. Data represent means ± SD, with $n = 3$ independent yeast colonies measured. $^{**}P \leq 0.01$ by Student's *t* test. (**F**) Fold change in the number of unsaturated bonds in fatty acids attached to triacylglycerides is shown. Lipids were extracted from *APOE3*- and *APOE4*-expressing human iPSC-derived astrocytes grown in astrocyte culture medium supplemented with CDP-choline (100 μM) or vehicle as control. Data represent means ± SD; $N = 3$ experiments. (**G**) Representative microscopy images of *APOE3*- and *APOE4*-expressing human iPSC-derived astrocytes stained with a Filipin III probe after culture in astrocyte medium supplemented with CDP-choline (100 μM) or vehicle as control. Quantification of Filipin III staining per cell ($N = 6$ to 7 experiments, with at least 20 cells imaged) is shown in the right panel. Data represent means ± SD. $^{**}P \leq 0.01$ and $^{***}P \leq 0.001$ by ANOVA.

iPSC-derived astrocytes with small-molecule inhibitors of diglyceride acyltransferases 1 and 2 (*63*, *64*) and observed a decrease in the lipid droplet number in the inhibitor-treated astrocytes compared with untreated astrocytes (Fig. 4B and fig. S5C). Therefore, *APOE4*-associated lipid defects may have arisen from the accumulation of endogenously synthesized lipids. Higher endogenous triacylglycerides and lipid droplet burden also suggested that *APOE4*-expressing human iPSC-derived astrocytes might present a genotype-specific sensitivity to challenge with exogenous lipids, as lipid droplets sequester FFAs into triacylglycerides to prevent lipotoxicity (*54*). Addition of the unsaturated fatty acid oleic acid to *APOE4*-expressing human iPSC-derived astrocytes in culture exacerbated lipid droplet accumulation (~3-fold) compared to *APOE3*-expressing human iPSC-derived astrocytes (Fig. 4C) (*26*), suggesting that *APOE4*-expressing human iPSC-derived astrocytes had reduced capacity to buffer excess lipids.

Choline supplementation reverses defective lipid homeostasis in human APOE4-expressing iPSC-derived astrocytes

Having shown that choline-stimulated synthesis of phosphatidylcholine restored lipid metabolism in *APOE4*-expressing yeast, we examined choline derivatives in metabolites extracted from our human iPSC-derived astrocytes. Similar to our observations in yeast, we found an increase in choline and glycerophosphocholine in *APOE4*-expressing astrocytes, suggesting an increased demand for uptake of choline and its metabolites (fig. S5D). Betaine, a choline derivative used in one-carbon metabolism but not in phosphatidylcholine synthesis, did not show changes in abundance between *APOE* genotypes (fig. S5D), suggesting that exogenously acquired choline metabolites were preferentially channeled toward phosphatidylcholine synthesis in *APOE4*-expressing astrocytes.

We then explored the effect of choline supplementation on *APOE4*-associated lipid perturbations in human iPSC-derived astrocytes in vitro. We cultured *APOE3* and *APOE4* isogenic astrocytes in either standard medium or medium supplemented with cytidine 5′-diphosphocholine (CDP-choline), a direct precursor of phosphatidylcholine synthesis by the Kennedy pathway (*65*). *APOE4*-expressing astrocytes treated with CDP-choline showed a decrease in lipid droplet number compared with that found in *APOE3*-expressing astrocytes (Fig. 4D). Furthermore, lipidomic profiling showed that CDP-choline treatment resulted in the reduction of total triacylglycerides in *APOE4* astrocytes (Fig. 4E). CDP-choline treatment also reduced the enrichment of unsaturated fatty acids in *APOE4* astrocytes

(Fig. 4F). These results confirmed that choline supplementation ameliorated the *APOE4*-induced lipid defects in human iPSC-derived astrocytes.

Choline supplementation rescues cholesterol accumulation associated with APOE4

Lipid droplets are composed not only of triacylglycerides but also of cholesterol and cholesterol esters (*30*, *54*). Cholesterol regulation plays a key role in *APOE*-related diseases including both cardiovascular disease and AD (*3*, *66*). We previously reported, using the fluorescent probe Filipin III (*67*), that *APOE4*-expressing astrocytes accumulate cholesterol (*27*). Cholesterol metabolism, including biosynthesis, efflux, and cholesterol storage in lipid droplets, is tuned to the cholesterol/phosphatidylcholine ratio in mammalian cells (*68*). We therefore used Filipin III to examine intracellular cholesterol in human iPSC-derived astrocytes treated with CDP-choline or vehicle in vitro. While vehicle-treated *APOE4*-expressing astrocytes accumulated more cellular cholesterol than *APOE3*-expressing astrocytes did, *APOE4* astrocyte cultures supplemented with CDP-choline did not show this defect (Fig. 4G).

DISCUSSION

Relating genetic polymorphisms to their phenotypic outcomes is key to understanding the molecular bases of disease risk and pathogenesis. In this study, we investigated the molecular basis of *APOE4*-associated lipid defects including an aberrant accumulation of unsaturated fatty acids and their storage in triglyceride-rich lipid droplets in human iPSC-derived astrocytes. Previous results in astrocytes from mice with human *APOE*-targeted replacement showed an increase in lipid droplets associated with the *APOE4* genotype (*26*). Another study (*3*) specifically examined the transcriptomic profiles of human iPSC-derived glia, human glia from postmortem AD patient brain tissue, and glia from mice with human *APOE*-targeted replacement. This study affirmed the central role of *APOE4* in perturbing lipid metabolism pathways in both humans and mice.

In our cellular models, we found several lipid metabolic nodes that could be manipulated to ameliorate lipid dysregulation in *APOE4*-expressing yeast cells and human iPSC-derived astrocytes. In particular, we discovered that stimulating phosphatidylcholine synthesis via the Kennedy pathway using exogenous choline supplementation was sufficient to reverse the *APOE4*-induced lipid defects in both yeast and human astrocytes while not impacting *APOE4* expression. A number of genetic associations support our findings. Compromised activity of the Kennedy pathway has been shown to result in accumulation of intracellular fats in humans and in mouse models bearing mutations in the *PCYT1A* gene (*69*, *70*). A genetic polymorphism in the *PEMT* gene that functions in an alternative phosphatidylcholine synthesis pathway has been associated with AD in a Chinese population (*71*).

APOE4-associated diseases have been linked to alterations in glucose and fatty acid metabolism (*72*, *73*). Lipid metabolism is an area of active investigation in research on aging and neurodegenerative diseases (*1*–*4*, *6*, *27*). AD-associated intracellular lipid accumulation has been reported in the postmortem brain tissue of AD patients (*5*), human fibroblasts (*74*), transgenic mouse models of AD (*5*), mouse primary neuronal cultures, and flies expressing *APOE4* (*75*).

Many lipid species have been implicated in neurotoxicity or selected as markers for early diagnosis of AD (*76*). Examination of a number of postmortem AD brains revealed a reduction in choline, ethanolamine, phosphatidylcholine, and phosphatidylethanolamine and an increase in their degradation products (*77*). Our data suggest that the *APOE4* genotype may impose an additional choline dependency, thus exacerbating the cholinergic deficit found in AD brains. In fact, our analysis of transcriptomes in postmortem brain tissue from *APOE4* carriers revealed that these individuals had increased expression of the high-affinity choline transporter *SLC44A1* (fig. S1F).

Over the last three decades, the link between age-related cognitive decline and compromised lipid metabolism has been increasingly appreciated. As a result, nutritional interventions aimed at elevating the synthesis of phospholipids became attractive as a non-invasive therapeutic strategy (*78*, *79*). CDP-choline itself has been previously proposed as a dietary supplement (*80*, *81*). In general, the demand for dietary choline may depend on multiple factors like age, ethnicity, and sex (*82*). For example, women tend to develop choline deficiency more often than do men (*65*). Women with an *APOE4* genotype show an increased risk of AD (*83*, *84*). Although most clinical trials for choline derivative supplementation in AD did not stratify individuals by *APOE* genotype, those that did noted greater efficacy of choline supplementation in *APOE4* populations than in those without the *APOE4* genotype (*85*). Our findings could point to a therapeutic strategy where choline supplementation is targeted to those with the *APOE4* genotype. Given that our study is limited to in vitro cell models, future research is required to expand our findings in animal models and *APOE4* carriers. For example, it would be interesting to examine how specific dietary changes affect brain metabolites and lipids in *APOE4* mouse models and human *APOE4* carriers and whether this impacts progression of *APOE4*-associated diseases. Such lines of research could identify early-stage markers of *APOE4*-dependent pathological states.

Lipid homeostasis affects many cellular processes, including membrane synthesis, vesicular trafficking, protein turnover, and cell proliferation (*86*). Our study suggests that *APOE4*'s status as a genetic risk factor for AD and other distinct diseases originates from the pleiotropic consequences of perturbed lipid metabolism characterized by increases in unsaturated triacylglycerides and a higher phosphatidylcholine requirement compared with the *APOE3* genotype. Our work provides a framework for understanding APOE4 function in disease risk and provides a rationale for genotype-specific dietary supplementation to diminish the detrimental consequences of the *APOE4* genetic polymorphism.

MATERIALS AND METHODS

Study design

The objective of this study was to establish the molecular consequences of the *APOE4* allele in yeast and human iPSC-derived astrocytes in vitro and to modulate these effects using chemical and genetic interventions. The study used *APOE3* and *APOE4* isogenic pairs of human iPSC-derived astrocytes and microglia, and yeast expressing human *APOE3* or *APOE4*. We measured the intracellular lipid content of yeast and human astrocytes using fluorescent probes and mass spectroscopy, and yeast growth after chemical and genetic perturbations. The sample sizes were selected on the basis of previous literature. The number of replications varied and is indicated in each figure legend. The study was not blinded.

Human iPSC-derived cell culture

iPSC-derived lines were generated from the parent line Coriell #AG09173 (female *APOE3/3* parental) and #AG10788 (female

APOE4/4 parental). Differentiation into astrocytes was performed as previously described (*27*). iPSCs were derived into microglia using a previously described protocol (*87*) with minor modifications.

Lipid droplet analysis

To assay the number of lipid droplets in astrocytes, an equal number of cells were plated on the 96-well μ-Plate (ibidi, 89626) in astrocyte medium or astrocyte medium supplemented with SCD1 inhibitor (A939572, 100 nM), inhibitors of DGAT1 (PF-04620110, 1 μM) and DGAT2 (PF-06424439, 1 μM), or CDP-choline (Sigma-Aldrich, 100 μM). After 12 to 14 days, cells were stained with LipidTox (Thermo Fisher Scientific/Molecular Probes) or Filipin III (Sigma-Aldrich) according to the manufacturer's protocols. To induce lipid droplet formation, astrocytes were incubated in the presence of oleic acid (Sigma-Aldrich, 20 μM) or vehicle (control). After 6 hours, the cells were carefully washed and stained with LipidTox, and proceeded as above. For lipid droplet count analysis in microglia, cells were plated at a density of 10,000 cells per well in a 96-well glass bottom plate (ibidi) in induced Microglia Base Medium (iMBM) medium prepared with custom Dulbecco's modified Eagle's medium/F12 lacking choline (Gibco) and supplemented with a low amount of choline chloride (Sigma-Aldrich, 15 μM). The cells were cultured for 2 weeks after plating without medium changes and were then fixed and stained using LipidTox Red (Thermo Fisher Scientific/Molecular Probes).

GTEx transcriptomic analysis

The genotypes of *APOE* ε4 (rs429358) for 838 subjects in the GTEx project (version 8) were extracted from vcf files (hg38) called from whole-genome sequencing data. Differential gene expression analysis of *APOE* ε4 (dichotomized into two groups, *APOE* $\varepsilon4^+$ and *APOE* $\varepsilon4^-$) was performed using DESeq2 (*88*) adjusted for RNA integrity number (RIN), age, sex, and five remove unwanted variation (RUV) components. The mean age of death of the sample is 57.56 ± 10.34 (SD). In addition, 68.8% of the individuals are male and 89.8% are white.

Yeast

S. cerevisiae strains were isogenic to the BY4741 background (MATa *his3Δ1 leu2Δ0 met15Δ0 ura3Δ0*). For the deletion of genes, a polymerase chain reaction product containing a selection cassette and short sequences for site-specific homologous recombination was transformed to yeast as described (*89*). Yeast were grown at 30°C in synthetic medium (SC) with YNB or nutrient-rich (YP) medium supplemented with 2% glucose (or 1% galactose only in fig. S2A and genetic screens). Yeast growth was measured using the Epoch 2 Microplate Spectrophotometer (BioTek) and quantified as an area under the growth curve within the 24 hours after induction starting at OD_{600} (optical density at 600 nm) = 0.1. Ole1p inhibitor ECC145 was produced by ChemBridge Co. (San Diego, CA, USA) and was added at indicated concentrations (10, 20, and 40 μM) to the synthetic medium containing β-estradiol (100 nM).

For genetic screens, we expressed APOE variants under galactose-inducible promoter. For screen validations and subsequent follow-up experiments, we adopted β-estradiol–inducible system that is independent on carbon source (*37*, *90*). We used this system to express APOE variants, TDP-43 and Aβ1-42. For the vast majority of experiments, we used β-estradiol at the 100 nM concentration, unless stated otherwise (e.g., to elicit a mild growth defect, and then 10 nM β-estradiol was applied). All the plasmids used in this study were deposited at Addgene (#78653).

Synthetic genetic array

Bait strains expressing APOE variants under galactose promoter, integrated either in the *LEU2* locus or on a centromeric plasmid, were engineered in the screening strain y7092 (gift from the Boone laboratory). Screens were performed as previously described (*39*, *91*).

Western blotting

The standard trichloroacetic acid precipitation-based method was used to extract protein from yeast. Precipitates were resuspended in HU buffer [8 M urea, 5% SDS, 1 mM EDTA, 1.5% dithiothreitol, 1% bromophenol blue, 200 mM tris-HCl (pH 6.8)] and incubated at 70°C for 15 min before loading on SDS–polyacrylamide gel electrophoresis (PAGE) gels. To separate proteins by SDS-PAGE, the 4 to 12% gradient bis-tris NuPAGE gels (Invitrogen) run in MES buffer were used. Gels were transferred to a nitrocellulose membrane using the iBlot2 system (Thermo Fisher Scientific). Primary antibodies were probed overnight followed by several washing steps and incubation with fluorescent secondary antibodies. Signal was measured using the LI-COR (Odyssey) system. Antibodies used in this study are as follows: anti-APOE (mouse monoclonal E8, Santa Cruz Biotechnology), anti-PGK1 (rabbit polyclonal, ABIN568371), anti-mouse secondary 800CW dye conjugate (LI-COR, 926-32212), and anti-rabbit secondary 680CW dye conjugate (LI-COR, 926-68073).

Lipidomic analysis

For lipid analysis, iPSC-derived astrocytes (derived from parental line; Coriell, #AG09173) were seeded in 10-cm dish for 12 to 14 days and grown in the astrocyte medium with 2% dialyzed fetal bovine serum and supplemented with vehicle or CDP-choline (100 μM). Yeast were grown in synthetic medium or synthetic medium supplemented with choline chloride (1 mM). The expression of APOE variants was induced with β-estradiol (100 nM) for 8 hours. Ten ODs equivalent of yeast were collected, washed twice with ice-cold ammonium bicarbonate, and resuspended in 1 ml of ammonium bicarbonate. Zirconia beads (Sigma-Aldrich) were added to mechanically disrupt cells using TissueLyser (Qiagen) (*28*). For both yeast and astrocytes, lipids were extracted using the Folch method (*92*).

Cytometry analysis after BODIPY 493/503 staining

Yeast strains were grown to saturation in synthetic medium with 2% glucose and subsequently diluted to OD_{600} = 0.1 in the synthetic medium containing β-estradiol (100 nM) for 8 hours. MACSQuant VYB cytometer with a 96-well plate platform (Miltenyi Biotec) was used to acquire 10,000 events in biological triplicates. The BODIPY 493/503 signal (green fluorescence) was measured with the B1 channel (525/50 filter), and median fluorescence values were calculated. Data were processed using FlowJo (FlowJo LLC).

Fluorescence microscopy

Yeast strains were grown to saturation in synthetic medium with 2% glucose and diluted to OD_{600} = 0.1 in the synthetic medium containing β-estradiol (100 nM) for 8 hours. Cells were diluted to OD_{600} of 0.2 in the same medium and transferred to a concanavalin A–coated 96-well plate. All images were acquired using a Nikon Eclipse Ti-E inverted microscope equipped with a Nikon Plan Apo 100× oil objective [numerical aperture (NA), 1.4] and a charge-coupled device (CCD) camera (Andor Technology). For all iPSC-derived cell type imaging, images were acquired using a Nikon Plan Apo 63× oil objective (NA, 1.4) using a Nikon Eclipse Ti-E inverted

microscope and a CCD camera (Andor Technology) or a Zeiss LSM710 inverted confocal microscope with a 40× water immersion objective and Z stacks with a stack height of 0.5 μm. Imaging was analyzed using Imaris (Bitplane) spot counting and area functions.

Statistical analysis

GraphPad Prism software was used to process data, calculate statistics, and prepare graphs. For determining statistical significance, we used the unpaired versions of *t* tests, unless stated otherwise. FlowJo was used to process fluorescence-activated cell sorting data. Images were processed using Imaris and Fiji (*93*).

SUPPLEMENTARY MATERIALS

stm.sciencemag.org/cgi/content/full/13/583/eaaz4564/DC1

Fig. S1. An increase in lipid droplets in human iPSC-derived *APOE4/APOE4* astrocytes and microglia.

Fig. S2. Yeast accumulate lipid droplets and lipid droplet–resident proteins upon expression of human *APOE4*.

Fig. S3. APOE4 expression in yeast leads to a growth defect in a dose-dependent manner.

Fig. S4. Choline supplementation rescues the *APOE4*-mediated growth defect in yeast.

Fig. S5. Analysis of lipid metabolism in human iPSC-derived *APOE4/APOE4* astrocytes.

Data file S1. Individual-level data for all figures.

View/request a protocol for this paper from *Bio-protocol*.

REFERENCES AND NOTES

1. S. Fanning, A. Haque, T. Imberdis, V. Baru, M. Inmaculada Barrasa, S. Nuber, D. Termine, N. Ramalingam, G. P. H. Ho, T. Noble, J. Sandoe, Y. Lou, D. Landgraf, Y. Freyzon, G. Newby, F. Soldner, E. Terry-Kantor, T.-E. Kim, H. F. Hofbauer, M. Becuwe, R. Jaenisch, D. Pincus, C. B. Clish, T. C. Walther, R. V. Farese Jr., S. Srinivasan, M. A. Welte, S. D. Kohlwein, U. Dettmer, S. Lindquist, D. Selkoe, Lipidomic analysis of α-synuclein neurotoxicity identifies stearoyl CoA desaturase as a target for Parkinson treatment. *Mol. Cell* **73**, 1001–1014.e8 (2019).
2. M. K. Shimabukuro, L. G. P. Langhi, I. Cordeiro, J. M. Brito, C. M. de Castro Batista, M. P. Mattson, V. de Mello Coelho, Lipid-laden cells differentially distributed in the aging brain are functionally active and correspond to distinct phenotypes. *Sci. Rep.* **6**, 23795 (2016).
3. J. TCW, S. A. Liang, L. Qian, N. H. Pipalia, M. J. Chao, Y. Shi, S. E. Bertelsen, M. Kapoor, E. Marcora, E. Sikora, D. M. Holtzman, F. R. Maxfield, B. Zhang, M. Wang, W. W. Poon, A. M. Goate, A. M. Goate, Cholesterol and matrisome pathways dysregulated in human *APOE* ε4 glia. bioRxiv 713362 [**Preprint**]. 25 July 2019.https://doi.org/10.1101/713362.
4. J. Marschallinger, T. Iram, M. Zardeneta, S. E. Lee, B. Lehallier, M. S. Haney, J. V. Pluvinage, V. Mathur, O. Hahn, D. W. Morgens, J. Kim, J. Tevini, T. K. Felder, H. Wolinski, C. R. Bertozzi, M. C. Bassik, L. Aigner, T. Wyss-Coray, Author Correction: Lipid-droplet-accumulating microglia represent a dysfunctional and proinflammatory state in the aging brain. *Nat. Neurosci.* **23**, 294 (2020).
5. L. K. Hamilton, M. Dufresne, S. E. Joppé, S. Petryszyn, A. Aumont, F. Calon, F. Barnabé-Heider, A. Furtos, M. Parent, P. Chaurand, K. J. L. Fernandes, Aberrant lipid metabolism in the forebrain niche suppresses adult neural stem cell proliferation in an animal model of Alzheimer's disease. *Cell Stem Cell* **17**, 397–411 (2015).
6. R. A. Stelzmann, H. N. Schnitzlein, F. R. Murtagh, An English translation of Alzheimer's 1907 paper, "über eine eigenartige erkankung der hirnrinde". *Clin. Anat.* **8**, 429–431 (1995).
7. T. L. Innerarity, R. W. Mahley, Enhanced binding by cultured human fibroblasts of apo-E-containing lipoproteins as compared with low density lipoproteins. *Biochemistry* **17**, 1440–1447 (1978).
8. R. W. Mahley, T. P. Bersot, V. S. Lequire, R. I. Levy, H. G. Windmueller, W. V. Brown, Identity of very low density lipoprotein apoproteins of plasma and liver Golgi apparatus. *Science* **168**, 380–382 (1970).
9. R. W. Mahley, Apolipoprotein E: Cholesterol transport protein with expanding role in cell biology. *Science* **240**, 622–630 (1988).
10. A. M. McIntosh, C. Bennett, D. Dickson, S. F. Anestis, D. P. Watts, T. H. Webster, M. B. Fontenot, B. J. Bradley, The apolipoprotein E (*APOE*) gene appears functionally monomorphic in chimpanzees (*Pan troglodytes*). *PLOS ONE* **7**, e47760 (2012).
11. J.-C. Lambert, S. Heath, G. Even, D. Campion, K. Sleegers, M. Hiltunen, O. Combarros, D. Zelenika, M. J. Bullido, B. Tavernier, L. Letenneur, K. Bettens, C. Berr, F. Pasquier, N. Fiévet, P. Barberger-Gateau, S. Engelborghs, P. De Deyn, I. Mateo, A. Franck, S. Helisalmi, E. Porcellini, O. Hanon; European Alzheimer's Disease Initiative Investigators, M. M. De Pancorbo, C. Lendon, C. Dufouil, C. Jaillard, T. Leveillard, V. Alvarez, P. Bosco, M. Mancuso, F. Panza, B. Nacmias, P. Boss, P. Piccardi, G. Annoni, D. Seripa, D. Galimberti, D. Hannequin, F. Licastro, H. Soininen, K. Ritchie, H. Blanché, J.-F. Dartigues, C. Tzourio, I. Gut, C. Van Broeckhoven, A. Alpérovitch, M. Lathrop, P. Amouyel, Genome-wide association study identifies variants at *CLU* and *CR1* associated with Alzheimer's disease. *Nat. Genet.* **41**, 1094–1099 (2009).
12. L. A. Farrer, L. A. Cupples, J. L. Haines, B. Hyman, W. A. Kukull, R. Mayeux, R. H. Myers, M. A. Pericak-Vance, N. Risch, C. M. van Duijn, Effects of age, sex, and ethnicity on the association between apolipoprotein E genotype and Alzheimer disease. A meta-analysis. APOE and Alzheimer Disease Meta Analysis Consortium. *JAMA* **278**, 1349–1356 (1997).
13. A. D. Roses, Apolipoprotein E alleles as risk factors in Alzheimer's disease. *Annu. Rev. Med.* **47**, 387–400 (1996).
14. J. Davignon, R. E. Gregg, C. F. Sing, Apolipoprotein E polymorphism and atherosclerosis. *Arteriosclerosis* **8**, 1–21 (1988).
15. C. F. Sing, P. P. Moll, Genetics of variability of CHD risk. *Int. J. Epidemiol.* **18**, S183–S195 (1989).
16. E. Torres-Perez, M. Ledesma, M. P. Garcia-Sobreviela, M. Leon-Latre, J. M. Arbones-Mainar, Apolipoprotein E4 association with metabolic syndrome depends on body fatness. *Atherosclerosis* **245**, 35–42 (2016).
17. K. M. Wright, K. A. Rand, A. Kermany, K. Noto, D. Curtis, D. Garrigan, D. Slinkov, I. Dorfman, J. M. Granka, J. Byrnes, N. Myres, C. A. Ball, J. G. Ruby, A prospective analysis of genetic variants associated with human lifespan. *G3* **9**, 2863–2878 (2019).
18. E. H. Corder, A. M. Saunders, W. J. Strittmatter, D. E. Schmechel, P. C. Gaskell, G. W. Small, A. D. Roses, J. L. Haines, M. A. Pericak-Vance, Gene dose of apolipoprotein E type 4 allele and the risk of Alzheimer's disease in late onset families. *Science* **261**, 921–923 (1993).
19. N. Zhao, C.-C. Liu, W. Qiao, G. Bu, Apolipoprotein E, receptors, and modulation of Alzheimer's disease. *Biol. Psychiatry* **83**, 347–357 (2017).
20. Y. Zhang, S. A. Sloan, L. E. Clarke, C. Caneda, C. A. Plaza, P. D. Blumenthal, H. Vogel, G. K. Steinberg, M. S. B. Edwards, G. Li, J. A. Duncan, S. H. Cheshier, L. M. Shuer, E. F. Chang, G. A. Grant, M. G. H. Gephart, B. A. Barres, Purification and characterization of progenitor and mature human astrocytes reveals transcriptional and functional differences with mouse. *Neuron* **89**, 37–53 (2016).
21. D. Petranovic, K. Tyo, G. N. Vemuri, J. Nielsen, Prospects of yeast systems biology for human health: Integrating lipid, protein and energy metabolism. *FEMS Yeast Res.* **10**, 1046–1059 (2010).
22. V. Khurana, S. Lindquist, Modelling neurodegeneration in *Saccharomyces cerevisiae*: Why cook with baker's yeast? *Nat. Rev. Neurosci.* **11**, 436–449 (2010).
23. A. H. Kachroo, J. M. Laurent, C. M. Yellman, A. G. Meyer, C. O. Wilke, E. M. Marcotte, Systematic humanization of yeast genes reveals conserved functions and genetic modularity. *Science* **348**, 921–925 (2015).
24. K. Natter, S. D. Kohlwein, Yeast and cancer cells—Common principles in lipid metabolism. *Biochim. Biophys. Acta* **1831**, 314–326 (2013).
25. J. K. Boyles, R. E. Pitas, E. Wilson, R. W. Mahley, J. M. Taylor, Apolipoprotein E associated with astrocytic glia of the central nervous system and with nonmyelinating glia of the peripheral nervous system. *J. Clin. Invest.* **76**, 1501–1513 (1985).
26. B. Farmer, J. Kluemper, L. Johnson, Apolipoprotein E4 alters astrocyte fatty acid metabolism and lipid droplet formation. *Cell* **8**, 182 (2019).
27. Y. T. Lin, J. Seo, F. Gao, H. M. Feldman, H. L. Wen, J. Penney, H. P. Cam, E. Gjoneska, W. K. Raja, J. Cheng, R. Rueda, O. Kritskiy, F. Abdurrob, Z. Peng, B. Milo, C. J. Yu, S. Elmsaouri, D. Dey, T. Ko, B. A. Yankner, L. H. Tsai, APOE4 causes widespread molecular and cellular alterations associated with Alzheimer's disease phenotypes in human iPSC-derived brain cell types. *Neuron* **98**, 1141–1154.e7 (2018).
28. O. L. Knittelfelder, S. D. Kohlwein, Lipid extraction from yeast cells. *Cold Spring Harb. Protoc.* **2017**, 408–411 (2017).
29. C. S. Ejsing, J. L. Sampaio, V. Surendranath, E. Duchoslav, K. Ekroos, R. W. Klemm, K. Simons, A. Shevchenko, Global analysis of the yeast lipidome by quantitative shotgun mass spectrometry. *Proc. Natl. Acad. Sci. U.S.A.* **106**, 2136–2141 (2009).
30. T. C. Walther, J. Chung, R. V. Farese Jr., Lipid droplet biogenesis. *Annu. Rev. Cell Dev. Biol.* **33**, 491–510 (2017).
31. T. K. Fam, A. S. Klymchenko, M. Collot, Recent advances in fluorescent probes for lipid droplets. *Materials* **11**, 1768 (2018).
32. B. K. Straub, B. Gyoengyoesi, M. Koenig, M. Hashani, L. M. Pawella, E. Herpel, W. Mueller, S. Macher-Goeppinger, H. Heid, P. Schirmacher, Adipophilin/perilipin-2 as a lipid droplet-specific marker for metabolically active cells and diseases associated with metabolic dysregulation. *Histopathology* **62**, 617–631 (2013).
33. D. V. Hansen, J. E. Hanson, M. Sheng, Microglia in Alzheimer's disease. *J. Cell Biol.* **217**, 459–472 (2018).
34. P. Singh, Budding yeast: An ideal backdrop for in vivo lipid biochemistry. *Front. Cell Dev. Biol.* **4**, 156 (2017).
35. R. W. Mahley, S. C. Rall Jr., Apolipoprotein E: Far more than a lipid transport protein. *Annu. Rev. Genomics Hum. Genet.* **1**, 507–537 (2000).

36. S. Treusch, S. Hamamichi, J. L. Goodman, K. E. S. Matlack, C. Y. Chung, V. Baru, J. M. Shulman, A. Parrado, B. J. Bevis, J. S. Valastyan, H. Han, M. Lindhagen-Persson, E. M. Reiman, D. A. Evans, D. A. Bennett, A. Olofsson, P. L. DeJager, R. E. Tanzi, K. A. Caldwell, G. A. Caldwell, S. Lindquist, Functional links between Aβ toxicity, endocytic trafficking, and Alzheimer's disease risk factors in yeast. *Science* **334**, 1241–1245 (2011).
37. A. Aranda-Díaz, K. Mace, I. Zuleta, P. Harrigan, H. El-Samad, Robust synthetic circuits for two-dimensional control of gene expression in yeast. *ACS Synth. Biol.* **6**, 545–554 (2017).
38. K. Athenstaedt, D. Zweytick, A. Jandrositz, S. D. Kohlwein, G. Daum, Identification and characterization of major lipid particle proteins of the yeast *Saccharomyces cerevisiae*. *J. Bacteriol.* **181**, 6441–6448 (1999).
39. A. H. Y. Tong, M. Evangelista, A. B. Parsons, H. Xu, G. D. Bader, N. Pagé, M. Robinson, S. Raghibizadeh, C. W. V. Hogue, H. Bussey, B. Andrews, M. Tyers, C. Boone, Systematic genetic analysis with ordered arrays of yeast deletion mutants. *Science* **294**, 2364–2368 (2001).
40. G. Giaever, A. M. Chu, L. Ni, C. Connelly, L. Riles, S. Véronneau, S. Dow, A. Lucau-Danila, K. Anderson, B. André, A. P. Arkin, A. Astromoff, M. El Bakkoury, R. Bangham, R. Benito, S. Brachat, S. Campanaro, M. Curtiss, K. Davis, A. Deutschbauer, K. D. Entian, P. Flaherty, F. Foury, D. J. Garfinkel, M. Gerstein, D. Gotte, U. Güldener, J. H. Hegemann, S. Hempel, Z. Herman, D. F. Jaramillo, D. E. Kelly, S. L. Kelly, P. Kötter, D. LaBonte, D. C. Lamb, N. Lan, H. Liang, H. Liao, L. Liu, C. Luo, M. Lussier, R. Mao, P. Menard, S. L. Ooi, J. L. Revuelta, C. J. Roberts, M. Rose, P. Ross-Macdonald, B. Scherens, G. Schimmack, B. Shafer, D. D. Shoemaker, S. Sookhai-Mahadeo, R. K. Storms, J. N. Strathern, G. Valle, M. Voet, G. Volckaert, C. yun Wang, T. R. Ward, J. Wilhelmy, E. A. Winzeler, Y. Yang, G. Yen, E. Youngman, K. Yu, H. Bussey, J. D. Boeke, M. Snyder, P. Philippsen, R. W. Davis, M. Johnston, Functional profiling of the *Saccharomyces cerevisiae* genome. *Nature* **418**, 387–391 (2002).
41. M. Costanzo, B. VanderSluis, E. N. Koch, A. Baryshnikova, C. Pons, G. Tan, W. Wang, M. Usaj, J. Hanchard, S. D. Lee, V. Pelechano, E. B. Styles, M. Billmann, J. Van Leeuwen, N. Van Dyk, Z. Y. Lin, E. Kuzmin, J. Nelson, J. S. Piotrowski, T. Srikumar, S. Bahr, Y. Chen, R. Deshpande, C. F. Kurat, S. C. Li, Z. Li, M. M. Usaj, H. Okada, N. Pascoe, B. J. S. Luis, S. Sharifpoor, E. Shuteriqi, S. W. Simpkins, J. Snider, H. G. Suresh, Y. Tan, H. Zhu, N. Malod-Dognin, V. Janjic, N. Przulj, O. G. Troyanskaya, I. Stagljar, T. Xia, Y. Ohya, A.-C. Gingras, B. Raught, M. Boutros, L. M. Steinmetz, C. L. Moore, A. P. Rosebrock, A. A. Caudy, C. L. Myers, B. Andrews, C. Boone, A global genetic interaction network maps a wiring diagram of cellular function. *Science* **353**, aaf1420 (2016).
42. M. A. Surma, C. Klose, D. Peng, M. Shales, C. Mrejen, A. Stefanko, H. Braberg, D. E. Gordon, D. Vorkel, C. S. Ejsing, R. Farese Jr., K. Simons, N. J. Krogan, R. Ernst, A lipid E-MAP identifies Ubx2 as a critical regulator of lipid saturation and lipid bilayer stress. *Mol. Cell* **51**, 519–530 (2013).
43. M. Schuldiner, S. R. Collins, N. J. Thompson, V. Denic, A. Bhamidipati, T. Punna, J. Ihmels, B. Andrews, C. Boone, J. F. Greenblatt, J. S. Weissman, N. J. Krogan, Exploration of the function and organization of the yeast early secretory pathway through an epistatic miniarray profile. *Cell* **123**, 507–519 (2005).
44. R. Covino, S. Ballweg, C. Stordeur, J. B. Michaelis, K. Puth, F. Wernig, A. Bahrami, A. M. Ernst, G. Hummer, R. Ernst, A eukaryotic sensor for membrane lipid saturation. *Mol. Cell* **63**, 49–59 (2016).
45. C.-W. Wang, S.-C. Lee, The ubiquitin-like (UBX)-domain-containing protein Ubx2/Ubxd8 regulates lipid droplet homeostasis. *J. Cell Sci.* **125**, 2930–2939 (2012).
46. N. Kolawa, M. J. Sweredoski, R. L. J. Graham, R. Oania, S. Hess, R. J. Deshaies, Perturbations to the ubiquitin conjugate proteome in yeast δubx mutants identify Ubx2 as a regulator of membrane lipid composition. *Mol. Cell. Proteomics* **12**, 2791–2803 (2013).
47. H. F. Hofbauer, F. H. Schopf, H. Schleifer, O. L. Knittelfelder, B. Pieber, G. N. Rechberger, H. Wolinski, M. L. Gaspar, C. O. Kappe, J. Stadlmann, K. Mechtler, A. Zenz, K. Lohner, O. Tehlivets, S. A. Henry, S. D. Kohlwein, Regulation of gene expression through a transcriptional repressor that senses acyl-chain length in membrane phospholipids. *Dev. Cell* **29**, 729–739 (2014).
48. L. S. Klig, M. J. Homann, G. M. Carman, S. A. Henry, Coordinate regulation of phospholipid biosynthesis in Saccharomyces cerevisiae: Pleiotropically constitutive opi1 mutant. *J. Bacteriol.* **162**, 1135–1141 (1985).
49. B. P. Young, J. J. H. Shin, R. Orij, J. T. Chao, S. C. Li, X. L. Guan, A. Khong, E. Jan, M. R. Wenk, W. A. Prinz, G. J. Smits, C. J. R. Loewen, Phosphatidic acid is a pH biosensor that links membrane biogenesis to metabolism. *Science* **329**, 1085–1088 (2010).
50. R. Burr, E. V. Stewart, W. Shao, S. Zhao, H. K. Hannibal-Bach, C. S. Ejsing, P. J. Espenshade, Mga2 transcription factor regulates an oxygen-responsive lipid homeostasis pathway in fission yeast. *J. Biol. Chem.* **291**, 12171–12183 (2016).
51. R. Chellappa, P. Kandasamy, C. S. Oh, Y. Jiang, M. Vemula, C. E. Martin, The membrane proteins, Spt23p and Mga2p, play distinct roles in the activation of Saccharomyces cerevisiae OLE1 gene expression. Fatty acid-mediated regulation of Mga2p activity is independent of its proteolytic processing into a soluble transcription activator. *J. Biol. Chem.* **276**, 43548–43556 (2001).
52. S. Zhang, Y. Skalsky, D. J. Garfinkel, *MGA2* or *SPT23* is required for transcription of the Δ9 fatty acid desaturase gene, *OLE1*, and nuclear membrane integrity in *Saccharomyces cerevisiae*. *Genetics* **151**, 473–483 (1999).
53. D. Xu, S. Sillaots, J. Davison, W. Hu, B. Jiang, S. Kauffman, N. Martel, P. Ocampo, C. Oh, S. Trosok, K. Veillette, H. Wang, M. Yang, L. Zhang, J. Becker, C. E. Martin, T. Roemer, Chemical genetic profiling and characterization of small-molecule compounds that affect the biosynthesis of unsaturated fatty acids in Candida albicans. *J. Biol. Chem.* **284**, 19754–19764 (2009).
54. J. A. Olzmann, P. Carvalho, Dynamics and functions of lipid droplets. *Nat. Rev. Mol. Cell Biol.* **20**, 137–155 (2019).
55. W. Fei, G. Shui, Y. Zhang, N. Krahmer, C. Ferguson, T. S. Kapterian, R. C. Lin, I. W. Dawes, A. J. Brown, P. Li, X. Huang, R. G. Parton, M. R. Wenk, T. C. Walther, H. Yang, A role for phosphatidic acid in the formation of "supersized" Lipid droplets. *PLOS Genet.* **7**, e1002201 (2011).
56. C. J. R. Loewen, M. L. Gaspar, S. A. Jesch, C. Delon, N. T. Ktistakis, S. A. Henry, T. P. Levine, Phospholipid metabolism regulated by a transcription factor sensing phosphatidic acid. *Science* **304**, 1644–1647 (2004).
57. S. A. Henry, S. D. Kohlwein, G. M. Carman, Metabolism and regulation of glycerolipids in the yeast *Saccharomyces cerevisiae*. *Genetics* **190**, 317–349 (2012).
58. M. Ramirez-Gaona, A. Marcu, A. Pon, A. C. Guo, T. Sajed, N. A. Wishart, N. Karu, Y. D. Feunang, D. Arndt, D. S. Wishart, YMDB 2.0: A significantly expanded version of the yeast metabolome database. *Nucleic Acids Res.* **45**, D440–D445 (2017).
59. R. J. Wurtman, M. Cansev, T. Sakamoto, I. H. Ulus, Use of phosphatide precursors to promote synaptogenesis. *Annu. Rev. Nutr.* **29**, 59–87 (2009).
60. N. D. Ridgway, The role of phosphatidylcholine and choline metabolites to cell proliferation and survival. *Crit. Rev. Biochem. Mol. Biol.* **48**, 20–38 (2013).
61. J. P. Fernández-Murray, M. H. Ngo, C. R. McMaster, Choline transport activity regulates phosphatidylcholine synthesis through choline transporter Hnm1 stability. *J. Biol. Chem.* **288**, 36106–36115 (2013).
62. Z. Xin, H. Zhao, M. D. Serby, B. Liu, M. Liu, B. G. Szczepankiewicz, L. T. J. Nelson, H. T. Smith, T. S. Suhar, R. S. Janis, N. Cao, H. S. Camp, C. A. Collins, H. L. Sham, T. K. Surowy, G. Liu, Discovery of piperidine-aryl urea-based stearoyl-CoA desaturase 1 inhibitors. *Bioorg. Med. Chem. Lett.* **18**, 4298–4302 (2008).
63. K. Futatsugi, D. W. Kung, S. T. M. Orr, S. Cabral, D. Hepworth, G. Aspnes, S. Bader, J. Bian, M. Boehm, P. A. Carpino, S. B. Coffey, M. S. Dowling, M. Herr, W. Jiao, S. Y. Lavergne, Q. Li, R. W. Clark, D. M. Erion, K. Kou, K. Lee, B. A. Pabst, S. M. Perez, J. Purkal, C. C. Jorgensen, T. C. Goosen, J. R. Gosset, M. Niosi, J. C. Pettersen, J. A. Pfefferkorn, K. Ahn, B. Goodwin, Discovery and optimization of imidazopyridine-based inhibitors of diacylglycerol acyltransferase 2 (DGAT2). *J. Med. Chem.* **58**, 7173–7185 (2015).
64. R. L. Dow, J.-C. Li, M. P. Pence, E. M. Gibbs, J. L. LaPerle, J. Litchfield, D. W. Piotrowski, M. J. Munchhof, T. B. Manion, W. J. Zavadoski, G. S. Walker, R. K. McPherson, S. Tapley, E. Sugarman, A. Guzman-Perez, P. DaSilva-Jardine, Discovery of PF-04620110, a potent, selective, and orally bioavailable inhibitor of DGAT-1. *ACS Med. Chem. Lett.* **2**, 407–412 (2011).
65. S. H. Zeisel, K.-A. da Costa, Choline: An essential nutrient for public health. *Nutr. Rev.* **67**, 615–623 (2009).
66. D. J. Gordon, J. L. Probstfield, R. J. Garrison, J. D. Neaton, W. P. Castelli, J. D. Knoke, D. R. Jacobs, S. Bangdiwala, H. A. Tyroler, High-density lipoprotein cholesterol and cardiovascular disease. Four prospective American studies. *Circulation* **79**, 8–15 (1989).
67. F. R. Maxfield, D. Wüstner, Analysis of cholesterol trafficking with fluorescent probes. *Methods Cell Biol.* **108**, 367–393 (2012).
68. T. A. Lagace, Phosphatidylcholine: Greasing the cholesterol transport machinery. *Lipid Insights* **8**, 65–73 (2015).
69. F. Payne, K. Lim, A. Girousse, R. J. Brown, N. Kory, A. Robbins, Y. Xue, A. Sleigh, E. Cochran, C. Adams, A. Dev Borman, D. Russel-Jones, P. Gorden, R. K. Semple, V. Saudek, S. O'Rahilly, T. C. Walther, I. Barroso, D. B. Savage, Mutations disrupting the Kennedy phosphatidylcholine pathway in humans with congenital lipodystrophy and fatty liver disease. *Proc. Natl. Acad. Sci. U.S.A.* **111**, 8901–8906 (2014).
70. D. E. Vance, J. E. Vance, Physiological consequences of disruption of mammalian phospholipid biosynthetic genes. *J. Lipid Res.* **50**, S132–S137 (2009).
71. X.-H. Bi, H.-L. Zhao, Z.-X. Zhang, J.-W. Zhang, PEMT G523A (V175M) is associated with sporadic Alzheimer's disease in a Chinese population. *J. Mol. Neurosci.* **46**, 505–508 (2012).
72. L. A. Johnson, E. R. S. Torres, S. Impey, J. F. Stevens, J. Raber, Apolipoprotein E4 and insulin resistance interact to impair cognition and alter the epigenome and metabolome. *Sci. Rep.* **7**, 43701 (2017).
73. T. Nuriel, S. L. Angulo, U. Khan, A. Ashok, Q. Chen, H. Y. Figueroa, S. Emrani, L. Liu, M. Herman, G. Barrett, V. Savage, L. Buitrago, E. Cepeda-Prado, C. Fung, E. Goldberg, S. S. Gross, S. A. Hussaini, H. Moreno, S. A. Small, K. E. Duff, Neuronal hyperactivity due to loss of inhibitory tone in APOE4 mice lacking Alzheimer's disease-like pathology. *Nat. Commun.* **8**, 1464 (2017).

74. M. D. Tambini, M. Pera, E. Kanter, H. Yang, C. Guardia-Laguarta, D. Holtzman, D. Sulzer, E. Area-Gomez, E. A. Schon, ApoE4 upregulates the activity of mitochondria-associated ER membranes. *EMBO Rep.* **17**, 27–36 (2016).
75. L. Liu, K. R. MacKenzie, N. Putluri, M. Maletić-Savatić, H. J. Bellen, The glia-neuron lactate shuttle and elevated ROS promote lipid synthesis in neurons and lipid droplet accumulation in glia via APOE/D. *Cell Metab.* **26**, 719–737.e6 (2017).
76. M. Mapstone, A. K. Cheema, M. S. Fiandaca, X. Zhong, T. R. Mhyre, L. H. Macarthur, W. J. Hall, S. G. Fisher, D. R. Peterson, J. M. Haley, M. D. Nazar, S. A. Rich, D. J. Berlau, C. B. Peltz, M. T. Tan, C. H. Kawas, H. J. Federoff, Plasma phospholipids identify antecedent memory impairment in older adults. *Nat. Med.* **20**, 415–418 (2014).
77. J. K. Blusztajn, I. L. Gonzalez-Coviella, M. Logue, J. H. Growdon, R. J. Wurtman, Levels of phospholipid catabolic intermediates, glycerophosphocholine and glycerophosphoethanolamine, are elevated in brains of Alzheimer's disease but not of Down's syndrome patients. *Brain Res.* **536**, 240–244 (1990).
78. C. W. Ritchie, J. Bajwa, G. Coleman, K. Hope, R. W. Jones, M. Lawton, M. Marven, P. Passmore, Souvenaid®: A new approach to management of early Alzheimer's disease. *J. Nutr. Health Aging* **18**, 291–299 (2014).
79. A. Caccamo, M. J. Huentelman, M. Naymik, N. Dave, R. Velazquez, W. Winslow, A. Tran, E. Ferreira, S. Oddo, I. S. Piras, Maternal choline supplementation ameliorates Alzheimer's disease pathology by reducing brain homocysteine levels across multiple generations. *Mol. Psychiatry* **25**, 2620–2629 (2020).
80. P. Grieb, Neuroprotective properties of citicoline: Facts, doubts and unresolved issues. *CNS Drugs* **28**, 185–193 (2014).
81. R. Conant, A. G. Schauss, Therapeutic applications of citicoline for stroke and cognitive dysfunction in the elderly: A review of the literature. *Altern. Med. Rev.* **9**, 17–31 (2004).
82. K.-A. Da Costa, K. D. Corbin, M. D. Niculescu, J. A. Galanko, S. H. Zeisel, Identification of new genetic polymorphisms that alter the dietary requirement for choline and vary in their distribution across ethnic and racial groups. *FASEB J.* **28**, 2970–2978 (2014).
83. S. C. Neu, J. Pa, W. Kukull, D. Beekly, A. Kuzma, P. Gangadharan, L. S. Wang, K. Romero, S. P. Arneric, A. Redolfi, D. Orlandi, G. B. Frisoni, R. Au, S. Devine, S. Auerbach, A. Espinosa, M. Boada, A. Ruiz, S. C. Johnson, R. Koscik, J. J. Wang, W. C. Hsu, Y. L. Chen, A. W. Toga, Apolipoprotein E genotype and sex risk factors for Alzheimer disease: A meta-analysis. *JAMA Neurol.* **74**, 1178–1189 (2017).
84. J. S. Damoiseaux, W. W. Seeley, J. Zhou, W. R. Shirer, G. Coppola, A. Karydas, H. J. Rosen, B. L. Miller, J. H. Kramer, M. D. Greicius, Gender modulates the *APOE* ε4 effect in healthy older adults: Convergent evidence from functional brain connectivity and spinal fluid tau levels. *J. Neurosci.* **32**, 8254–8262 (2012).
85. X. A. Alvarez, R. Mouzo, V. Pichel, P. Pérez, M. Laredo, L. Fernández-Novoa, L. Corzo, R. Zas, M. Alcaraz, J. J. Secades, R. Lozano, R. Cacabelos, Double-blind placebo-controlled study with citicoline in APOE genotyped Alzheimer's disease patients. Effects on cognitive performance, brain bioelectrical activity and cerebral perfusion. *Methods Find. Exp. Clin. Pharmacol.* **21**, 633–644 (1999).
86. T. Harayama, H. Riezman, Understanding the diversity of membrane lipid composition. *Nat. Rev. Mol. Cell Biol.* **19**, 281–296 (2018).
87. A. McQuade, M. Coburn, C. H. Tu, J. Hasselmann, H. Davtyan, M. Blurton-Jones, Development and validation of a simplified method to generate human microglia from pluripotent stem cells. *Mol. Neurodegener.* **13**, 67 (2018).
88. M. I. Love, W. Huber, S. Anders, Moderated estimation of fold change and dispersion for RNA-seq data with DESeq2. *Genome Biol.* **15**, 550 (2014).
89. C. Janke, M. M. Magiera, N. Rathfelder, C. Taxis, S. Reber, H. Maekawa, A. Moreno-Borchart, G. Doenges, E. Schwob, E. Schiebel, M. Knop, A versatile toolbox for PCR-based tagging of yeast genes: New fluorescent proteins, more markers and promoter substitution cassettes. *Yeast* **21**, 947–962 (2004).
90. R. S. McIsaac, B. L. Oakes, X. Wang, K. A. Dummit, D. Botstein, M. B. Noyes, Synthetic gene expression perturbation systems with rapid, tunable, single-gene specificity in yeast. *Nucleic Acids Res.* **41**, e57 (2013).
91. E. Kuzmin, M. Costanzo, B. Andrews, C. Boone, Synthetic genetic array analysis. *Cold Spring Harb. Protoc.* **2016**, 359–372 (2016).
92. J. Folch, M. Lees, G. H. SLOANE STANLEY, A simple method for the isolation and purification of total lipides from animal tissues. *J. Biol. Chem.* **226**, 497–509 (1957).
93. J. Schindelin, I. Arganda-Carreras, E. Frise, V. Kaynig, M. Longair, T. Pietzsch, S. Preibisch, C. Rueden, S. Saalfeld, B. Schmid, J.-Y. Tinevez, D. J. White, V. Hartenstein, K. Eliceiri, P. Tomancak, A. Cardona, Fiji: An open-source platform for biological-image analysis. *Nat. Methods* **9**, 676–682 (2012).

Acknowledgments: This work is dedicated to our inspiring mentor Susan Lindquist. We thank members of the Lindquist, Tsai, and Sabatini laboratories for helpful suggestions. We thank P. Thiru for technical assistance with bioinformatics, Y.-T. Lin for help with iPSC lines and sharing of transcriptomic data, and J. Valderrain for analysis of large-scale datasets. We thank D. Jarosz, D. Pincus, P. Tsvetkov, J. Rettenmaier, M. Maresca, M. Bohlooly, L. Clayton, and B. Bevis for suggestions. **Funding:** G.S. was supported by an EMBO Fellowship (ALTF 829-2015) and was an HHMI fellow of the Helen Hay Whitney Foundation. P.N. was supported by the Helen Hay Whitney Foundation, by an NIH/NIA K99 award (AG055697-03), and by the Intramural Research Program of the NIH/NIDDK. N.K. is an HHMI fellow of the Damon Runyon Foundation. D.M.S. is supported by an NIH/NCI grant (R01 CA103866). He is an investigator of the Howard Hughes Medical Institute and an American Cancer Society Research Professor. The work in the Lindquist and Tsai laboratories was supported by the Neurodegeneration Consortium, the Robert A. and Renee E. Belfer Foundation, the Howard Hughes Medical Institute, the Ludwig Family Foundation, support from Kara and Stephen Ross, and NIH grants RF1 AG048029, RF1 AG062377, U01 NS110453, R01 AG062335, and R01 AG058002 (to L.-H.T.). The GTEx Project was supported by the Common Fund of the Office of the Director of the NIH and by NCI, NHGRI, NHLBI, NIDA, NIMH, and NINDS. **Author contributions:** G.S., P.N., L.-H.T., and S.L. conceptualized the study. G.S. performed yeast screens, yeast genetics, and choline rescue experiments. G.S., P.N., and J.M.B. performed experiments with astrocytes and microglia and performed culture medium analysis, with the help of W.T.R., A.A.A., L.A., E.L., B.M., A.G., and V.B. G.S. and P.N. performed lipid analysis with the help of S.B., N.K., and C.A.L. L.H. and M.K. analyzed transcriptomic data. G.S. and P.N. wrote the original draft, and J.M.B., M.K., D.M.S., and L.-H.T. edited it. **Competing interests:** S.L. is a cofounder of Yumanity Therapeutics. L.-H.T. is a member of the Scientific Advisory Board of Yumanity Therapeutics. P.N. and S.L. are coinventors on U.S. Patent PCT/US2015/049674 "Cells expressing apolipoprotein E and uses thereof." G.S., P.N., J.M.B., and L.-H.T. are coinventors on patent application 63/023,698 "Use of choline supplementation as therapy for APOE4-related disorders." G.S. and A.A.A. are currently employees and shareholders of AstraZeneca. C.A.L. is a paid consultant for ReviveMed Inc. **Data and materials availability:** Plasmids used in the study have been deposited at Addgene with accession number 78653.

Submitted 10 September 2019
Resubmitted 27 May 2020
Accepted 5 November 2020
Published 3 March 2021
10.1126/scitranslmed.aaz4564

Citation: G. Sienski, P. Narayan, J. M. Bonner, N. Kory, S. Boland, A. A. Arczewska, W. T. Ralvenius, L. Akay, E. Lockshin, L. He, B. Milo, A. Graziosi, V. Baru, C. A. Lewis, M. Kellis, D. M. Sabatini, L.-H. Tsai, S. Lindquist, *APOE4* disrupts intracellular lipid homeostasis in human iPSC-derived glia. *Sci. Transl. Med.* **13**, eaaz4564 (2021).

Science Translational Medicine

APOE4 disrupts intracellular lipid homeostasis in human iPSC-derived glia

Grzegorz SienskiPriyanka NarayanJulia Maeve BonnerNora KorySebastian BolandAleksandra A. ArczewskaWilliam T. RalveniusLeyla AkayElana LockshinLiang HeBlerta MiloAgnese GraziosiValeriya BaruCaroline A. LewisManolis KellisDavid M. SabatiniLi-Huei TsaiSusan Lindquist

Sci. Transl. Med., 13 (583), eaaz4564. • DOI: 10.1126/scitranslmed.aaz4564

APOE4 disrupts lipid homeostasis in glia

APOE4 is a strong genetic risk factor for many diseases, most notably, late-onset Alzheimer's disease. Sienski *et al.* now show that cultured human glia with an *APOE4* genotype accumulated unsaturated triglycerides leading to a lipid imbalance. Using genetic screens in yeast, the authors discovered that promoting phospholipid synthesis through choline supplementation of culture medium restored a normal lipid state in *APOE4*-expressing yeast cells. The authors then demonstrated that choline supplementation also restored lipid homeostasis in human *APOE4* astrocytes. These findings suggest that modulating glial metabolism could help to reduce *APOE4*-associated disease risk.

Science Translational Medicine (ISSN 1946-6242) is published by the American Association for the Advancement of Science. 1200 New York Avenue NW, Washington, DC 20005. The title *Science Translational Medicine* is a registered trademark of AAAS.